


Research Article

Folic Acid-Conjugated Silica-Modified $\text{TbPO}_4 \cdot \text{H}_2\text{O}$ Nanorods for Biomedical Applications

Le Thi Vinh,¹ Tran Thu Huong ,^{2,3} Ha Thi Phuong,⁴ Hoang Thi Khuyen,^{2,3} Nguyen Manh Hung,¹ Do Thi Thao,⁵ and Le Quoc Minh⁶

¹Faculty of Basic Science, Hanoi University of Mining and Geology, 18-Pho Vien, Hanoi, Vietnam

²Institute of Materials Science, Vietnam Academy of Science and Technology, 18 Hoang Quoc Viet, Hanoi, Vietnam

³Graduate University of Science and Technology, Vietnam Academy of Science and Technology, 18 Hoang Quoc Viet, Hanoi, Vietnam

⁴Department of Chemistry, Hanoi Medical University, 1-Ton That Tung, Hanoi, Vietnam

⁵Institute of Biotechnology, Vietnam Academy of Science and Technology, 18-Hoang Quoc Viet, Hanoi, Vietnam

⁶Institute of Theoretical and Applied Research, Duy Tan University, 1 Phung Chi Kien, Hanoi, Vietnam

Correspondence should be addressed to Tran Thu Huong; tthuongims@gmail.com

Received 28 May 2021; Revised 10 August 2021; Accepted 28 September 2021; Published 28 October 2021

Academic Editor: Scott L. Wallen

Copyright © 2021 Le Thi Vinh et al. This is an open access article distributed under the Creative Commons Attribution License, which permits unrestricted use, distribution, and reproduction in any medium, provided the original work is properly cited.

We report on the synthesis and characterization of folic acid-conjugated silica-modified $\text{TbPO}_4 \cdot \text{H}_2\text{O}$ nanorods for biomedical applications. The uniform shape $\text{TbPO}_4 \cdot \text{H}_2\text{O}$ nanorods with a hexagonal phase were successfully synthesized by wet chemical methods. A novel $\text{TbPO}_4 \cdot \text{H}_2\text{O} @ \text{silica-NH}_2$ nanocomplex was then formed by functionalizing these nanorods with silica and conjugating with biological agents. The field emission scanning electron microscopy, energy-dispersive X-ray, and X-ray diffraction reveal the morphology and structure of the nanorods, with their controllable sizes (500-800 nm in length and 50-80 nm in diameter). The Fourier transform infrared spectroscopy was employed to identify chemical substances or functional groups of the $\text{TbPO}_4 \cdot \text{H}_2\text{O} @ \text{silica-NH}_2$ nanocomplex. The photoluminescence spectra show the four emission lines of $\text{TbPO}_4 \cdot \text{H}_2\text{O} @ \text{silica-NH}_2$ in folic acid at 488, 540, 585, and 621 nm under 355 nm laser excitation, which could be attributed to the $^5\text{D}_4 \rightarrow ^7\text{F}_j$ ($J = 6, 5, 4, 3$) transitions of Tb^{3+} . The $\text{TbPO}_4 \cdot \text{H}_2\text{O} @ \text{silica-NH}_2$ nanorods were conjugated with folic acid for the detection of MCF7 breast cancer cells. The obtained results show a promising possibility for the recognition of living cells that is of crucial importance in biolabeling.

1. Introduction

Rare earth containing luminescent nanophosphors with many advantages such as high stability, strong luminescence, noncomplex fabrication, easy surface functionalization, and friendly to environment and human body have been very promising materials for healthcare application, especially for biomedical fluorescence labeling [1–10]. Recently, the development of rare earth containing luminescent nanorods for application in biomedicine is attracted topic for scientists in materials science field [11–15]. According to some previous studies, compared with nanospheres, nanorods could have a short coherent time in the interband transitions.

Therefore, the decay time of nanorods is relatively long that allows for more stable luminescence intensity.

Additionally, the nanorods indicate very small radiation damping because of small volumes [16, 17]. Besides, nanorods are also very interest for scientific community because the morphology is related with an intrinsic multifunction arising in different contact areas [18]. These characteristics are also very useful potential objects for application in highly functional devices. Some rare earth containing luminescent nanorods could be synthesized by wet chemical routes [19–21] including our successful work with TbPO_4 nanorods [22]. These results and some other previous studies have shown that the morphology of materials can have

important impacts on luminescent intensity. In biomedical applications, high luminescent yield with nanosize and biomedical compatibility is still required as indispensable property for biolabeling materials. Therefore, it is necessary for the development of a stable and high-quality synthesized procedure to fabricate a higher luminescent intensity of $\text{TbPO}_4 \cdot \text{H}_2\text{O}$ nanorods with possible ability in biomedical application.

Folates are salts of folic acid. Folate is also the name of the anionic form of folic acid, and it has a high-affinity binding reagent that could recognize folate receptor. Moreover, folic acid is founded to many promises due to low cost, high stability, its faster internalization kinetics through cellular membrane, and its nonimmunogenicity. Coupling of folates to nanomaterials advanced their cellular uptake by folate receptor mediated endocytosis which can avoid their non-specific attacks to normal tissues, also which can increase their cellular uptake within target cells. Folic acid was attached to the $\text{TbPO}_4 \cdot \text{H}_2\text{O}$ @silica- NH_2 nanorods via the formation of amide linkage between the amine group of $\text{TbPO}_4 \cdot \text{H}_2\text{O}$ @silica- NH_2 nanorods and the carboxyl group of folic acid.

In this work, we focus on the development of $\text{TbPO}_4 \cdot \text{H}_2\text{O}$ nanorods prepared by wet chemical methods with strong luminescent that is potential for biolabeling application. The $\text{TbPO}_4 \cdot \text{H}_2\text{O}$ nanorods were covered by a silica layer, attached with amine groups, and then linked with folic acid by a coupling reaction to form the $\text{TbPO}_4 \cdot \text{H}_2\text{O}$ @silica- NH_2 nanocomplex. The nanocomplex optical properties were discussed in detail. The biocomplex emitted strongly in green at 540 nm. The primary test result showed that $\text{TbPO}_4 \cdot \text{H}_2\text{O}$ @silica- NH_2 -folic acid nanocomplex could be used for both detection and recognition of MCF7 breast cancer cells.

2. Experimental Procedure

2.1. Materials. Terbium (III) nitrate pentahydrate ($\text{Tb}(\text{NO}_3)_3 \cdot 5\text{H}_2\text{O}$) (Aldrich, 99.9%), ammonium dihydrogen phosphate ($\text{NH}_4\text{H}_2\text{PO}_4$) (Merck, 99%), sodium hydroxide (NaOH) (Merck, 99%), tetraethyl orthosilicate (Merck, 99%), 3-aminopropyltriethoxysilane (Aldrich, 98%), dimethyl sulfoxide (Aldrich, 99.9%) with N-hydroxysuccinimide (Aldrich, 98%), N,N'-dicyclohexylcarbodiimide (Aldrich, 99%), and folic acid ($\text{C}_{19}\text{H}_{19}\text{N}_7\text{O}_6$).

2.2. Synthesis of $\text{TbPO}_4 \cdot \text{H}_2\text{O}$ Nanorods. Wet chemical methods which include hydrothermal, sol-gel, and coprecipitation synthesis were developed to obtain ultrafine, very homogeneous, and high purity powders. Among these various wet chemical synthesis methods, hydrothermal method is a very simple method with cost effectiveness, easy control over material size, and compositions. Figure 1 illustrates the scheme of synthesis procedure by hydrothermal method for $\text{TbPO}_4 \cdot \text{H}_2\text{O}$ nanorods.

The $\text{TbPO}_4 \cdot \text{H}_2\text{O}$ nanorods were synthesized as the following procedure. 15 ml (0.05 M) terbium (III) nitrate pentahydrate and 225 ml (0.05 M) ammonium dihydrogen phosphate were mixed in stirred vigorously solution. After-

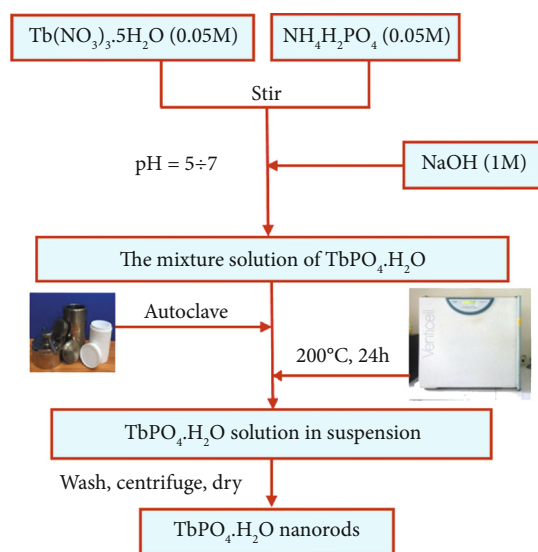


FIGURE 1: The schematic for the hydrothermal process of the $\text{TbPO}_4 \cdot \text{H}_2\text{O}$ nanorods.

ward, sodium hydroxide was added slowly to the solution and stirred using a magnetic pellet for 6 hours with adjusted pH in the range of 5 ÷ 7. Meanwhile, the reactant $\text{Tb}^{3+}/\text{PO}_4^{3-}$ molar ratio was changed from 1/15 to 1/1 by increasing the amount of terbium nitrate. Next, the mixture solution was put in a Teflon-lined stainless-steel autoclave and heated up at 200°C for 24 hours. The $\text{TbPO}_4 \cdot \text{H}_2\text{O}$ was separated by centrifuge at 5800 rpm. The achieved product had been washed several times by deionized water and dried at 60°C for 6-24 hours.

2.3. Synthesis of $\text{TbPO}_4 \cdot \text{H}_2\text{O}$ @Silica and $\text{TbPO}_4 \cdot \text{H}_2\text{O}$ @Silica- NH_2 Nanorods. Silica coating is a strategy for inorganic surface treatment to make nanorods water-dispersible and biocompatible as well as to introduce new therapeutic functionalities when using silica to entrap a therapeutic agent and deliver it to the treatment destination. Silica is highly stable, biocompatible, and optically transparent. When it is utilized as a coating material, surface silanization can flexibly offer abundant functional groups (e.g., $-\text{COOH}$, $-\text{NH}_2$, and $-\text{SH}$), allowing for conjugation with biomolecules and exploiting the optical properties of functionalized materials.

$\text{TbPO}_4 \cdot \text{H}_2\text{O}$ @silica nanorods were prepared by sol-gel Stöber process as the following: (i) 5 ml of tetraethyl orthosilicate, 5 ml of ethanol, 0.5 ml of acetic acid, and 1 ml of deionized water were stirred and mixed at room temperature for 6 hours (solution 1); (ii) then, 20 ml of as-synthesized $\text{TbPO}_4 \cdot \text{H}_2\text{O}$ solution were dispersed in a mixed solution of 20 ml ethanol and 1 ml deionized water using a vortex mixer for 30 minutes (solution 2). Solution 2 was slowly dripped into solution 1; then, the mixture had been continuously stirred for 24 hours. The $\text{TbPO}_4 \cdot \text{H}_2\text{O}$ @silica was achieved as a result of the separation using centrifugation. The product was washed and dried at 60°C for 20 hours.

$\text{TbPO}_4 \cdot \text{H}_2\text{O}$ @silica- NH_2 nanorods were prepared as the following: $\text{TbPO}_4 \cdot \text{H}_2\text{O}$ @silica mixed with 20 ml of ethanol,

3 ml of 3-aminopropyltriethoxysilane, and 1 ml of tetraethyl orthosilicate was poured in a three-necked flask (size 50 ml) by stirring with a magnetic pellet for 60 minutes. This solution was heated up to 60°C in the reflux during continuous stirring for 20 hours. Finally, $\text{TbPO}_4 \cdot \text{H}_2\text{O}@\text{silica-NH}_2$ products were separated by centrifuge, then washed with deionized water and dried again.

2.4. Conjugation of $\text{TbPO}_4 \cdot \text{H}_2\text{O}@\text{Silica-NH}_2$ Nanorods with Folic Acid. The conjugation procedure of $\text{TbPO}_4 \cdot \text{H}_2\text{O}@\text{silica-NH}$ -folic acid was prepared as the following. First, 0.5 mg folic acid was dissolved in 15 ml of dimethyl sulfoxide with N-hydroxysuccinimide (NHS) in the presence of N,N'-dicyclohexylcarbodiimide (DCC) at room temperature by using a vortex mixer for 30 minutes (the molar ratio of folic acid/NHS/DCC is 1/5/3). After that, this activated folic acid was continuously stirred in the darkness for 20 hours. Next, 10 ml dispersed $\text{TbPO}_4 \cdot \text{H}_2\text{O}@\text{silica-NH}_2$ nanorods in ethanol have been mixed in the above-activated folic acid solution. The mixed solution was continuously stirred again in the darkness for 20 hours. The final conjugated $\text{TbPO}_4 \cdot \text{H}_2\text{O}@\text{silica-NH}$ -folic acid product was filtrated and separated by the centrifuge with rotation speed of 5800 rpm.

2.5. Cell Culture Experiments. The MCF7 breast cancer cell line was kindly provided by Dr. J M Pezzuto-US. They were cultured in MEME medium (Sigma Chemical Co.) and supplemented with 10% bovine embryonic serum (FBS) (Sigma Chemical Co.) and 50 $\mu\text{g}/\text{ml}$ gentamicin. Cells were inoculated after 3-5 days and incubated in an incubator at 37°C and 5% CO_2 .

The biocomplex $\text{TbPO}_4 \cdot \text{H}_2\text{O}@\text{silica-NH}$ -folic acid and the MCF7 breast cancer cells were seeded in 24-well plates with a density of $10^4 \text{ cells}\cdot\text{ml}^{-1}$; then, these biological samples have been incubated for 24 hours. Polyethylene glycol 1500 (Sigma) and the biocomplex $\text{TbPO}_4 \cdot \text{H}_2\text{O}@\text{silica-NH}$ -folic acid with the concentration of 20 $\mu\text{g}/\text{ml}$ were supplemented to the cell-seeded wells for 6 hours. Finally, remove the cultured medium; the fixed time cells and MCF7 breast cancer cells were poured in falcon tubes (size of 15 ml). Then, the achieved product was cleaned by phosphate buffer saline three times. Fluorescent images have been observed by an Olympus Scan[^]R 100X fluorescent microscope.

2.6. Characterization Techniques. The morphology and structure of the synthesized nanorods have been investigated by a Field Emission Scanning Electron Microscope (FE-SEM Hitachi S-4800), X-ray diffractometer (XRD) using a Siemens D5000 with CuK_α radiation ($\lambda = 1.5406 \text{ \AA}$ in the 2-theta range of $10^\circ \leq 2\theta \leq 80^\circ$), and energy-dispersive X-ray (EDX). The chemical substances or functional groups of the $\text{TbPO}_4 \cdot \text{H}_2\text{O}@\text{silica-NH}_2$ have been identified by Fourier transform infrared spectroscopy (FTIR NEXUS 670). The photoluminescence spectroscopy (Horiba iHR550 setup) has been used for photoluminescence property characterization of the synthesized biological nanosamples. The cells were observed under an Olympus Scan[^]R fluorescence microscope (Olympus Europa SE & Co.KG, Hamburg, DE).

3. Results and Discussion

3.1. The Morphology of Synthesized Samples and Energy-Dispersive X-Ray Analysis. Figures 2(a)–2(e) show FESEM images of $\text{TbPO}_4 \cdot \text{H}_2\text{O}$ nanophosphors with the different reactant $\text{Tb}^{3+}/\text{PO}_4^{3-}$ molar ratios and $\text{TbPO}_4 \cdot \text{H}_2\text{O}@\text{silica-NH}_2$ nanophosphors. These images provide information for the morphological analysis of the synthesized samples. It was observed from the FE-SEM images that the samples are formed in the nanorod shapes with molar ratios of $\text{Tb}^{3+}/\text{PO}_4^{3-}$ which are 1/15, 1/10, 1/5, and 1/1. The shape of these nanorods is very uniform proving the stable synthesized procedure. The size of synthesized nanorod can be estimated in the range of 20-30 nm in diameter and 200-300 nm in length from Figures 2(a) and 2(b). The reactant $\text{Tb}^{3+}/\text{PO}_4^{3-}$ molar ratio for the products of Figures 2(a) and 2(b) is 1/15 and 1/10, respectively. When these molar ratios are increased to 1/5 and 1/1, the as-synthesized TbPO_4 exhibits more uniform nanorod morphology (Figures 2(c) and 2(d), respectively). The length of nanorods increases in the range of 300-500 nm, and their observed diameters are bigger in the range of 30 to 50 nm with the same reaction time. We produce $\text{TbPO}_4 \cdot \text{H}_2\text{O}$ nanorod biomedical nanocomposite complexes by several steps. First, it is necessary to treat the surface of the nanorods. Then, we functionalized the samples with amine groups. Finally, conjugation with biological agents of nanocomposite complexes has been done.

Currently, silica coating is the main inorganic surface treatment. The silica shell may offer sites for the loading of functional molecules and allows the $-\text{NH}_2$, $-\text{COOH}$, or $-\text{SH}$ functionalization necessary for further chemical reaction with biological molecules and other functionalized compounds. Therefore, because of its versatility, silica constitutes an excellent intermediate layer, which allows the combination of $\text{TbPO}_4 \cdot \text{H}_2\text{O}$ nanorods and additional molecules that need to be kept separate from one another. In these results, the nanorods with a 1/1 mole ratio of $\text{Tb}^{3+}/\text{PO}_4^{3-}$ have been chosen for the next study including protection with silica and functionalization with amine. After $\text{TbPO}_4 \cdot \text{H}_2\text{O}$ nanorods are protected with silica and attached with amine groups (forming $\text{TbPO}_4 \cdot \text{H}_2\text{O}@\text{silica-NH}_2$ samples), the sizes of the products are slightly increasing with diameters in the range of 50-80 nm and lengths in the range of 500-800 nm (see Figure 2(e)).

The nanorods of $\text{TbPO}_4 \cdot \text{H}_2\text{O}$ and $\text{TbPO}_4 \cdot \text{H}_2\text{O}@\text{silica-NH}_2$ analyzed the elemental composition on material surfaces by energy-dispersive X-ray technique (EDX). The results of these analyses are shown in Figure 3. We can see the presence of Tb, P, and O in the EDX spectrum as the basic elements in original nanorods (Figure 3(a)). Obviously, the additional Si and N peaks have been observed in the EDX spectrum of silica-coated samples with the amine functionalized group (Figure 3(b)). The EDX analysis confirms that there are no other impurities detected in the analyzed nanorods (both are original and functionalized samples).

3.2. The Fourier Transform Infrared Spectra and Crystalline Phase Identification. The Fourier transform infrared spectrum of the nanorods of $\text{TbPO}_4 \cdot \text{H}_2\text{O}$ (1) and

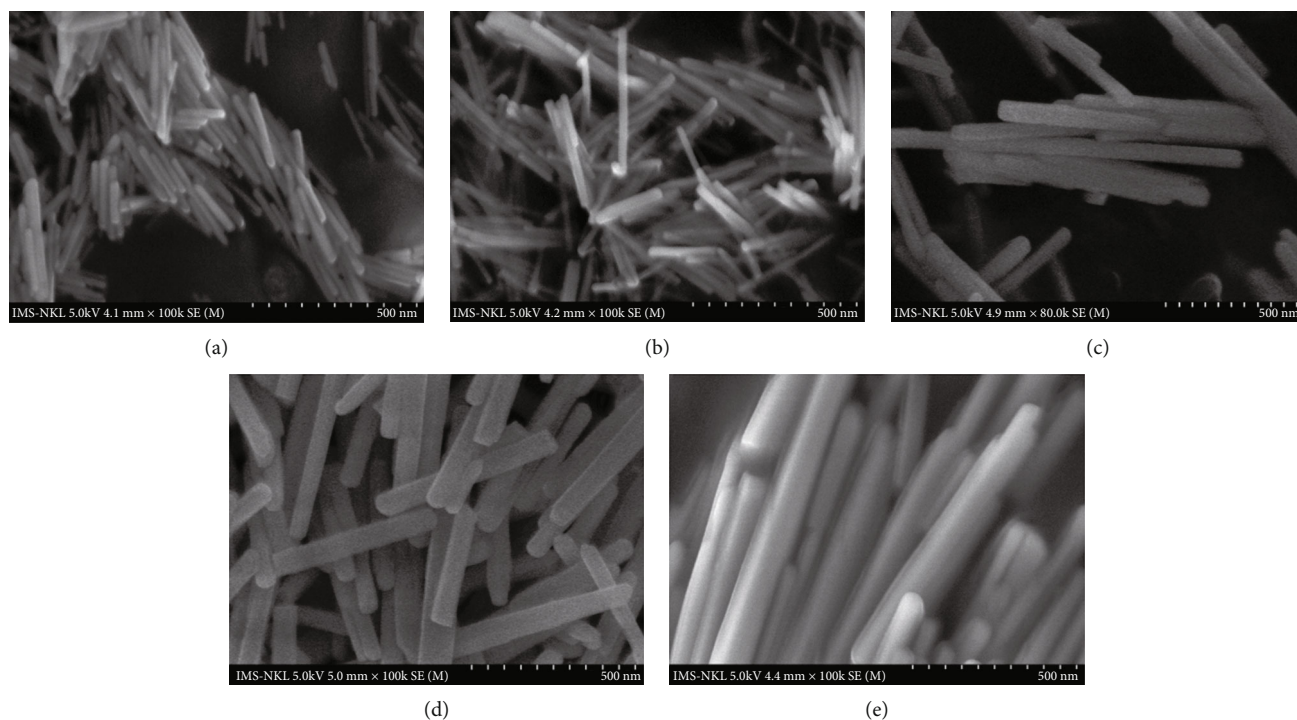


FIGURE 2: FESEM images of the $\text{TbPO}_4 \cdot \text{H}_2\text{O}$ samples with molar ratios of $\text{Tb}^{3+}/\text{PO}_4^{3-}$ are (a) 1/15, (b) 1/10, (c) 1/5, (d) 1/1, and (e) nanocomplexes protected with silica and attached with amine groups (molar ratio of $\text{Tb}^{3+}/\text{PO}_4^{3-}$ is 1/1).

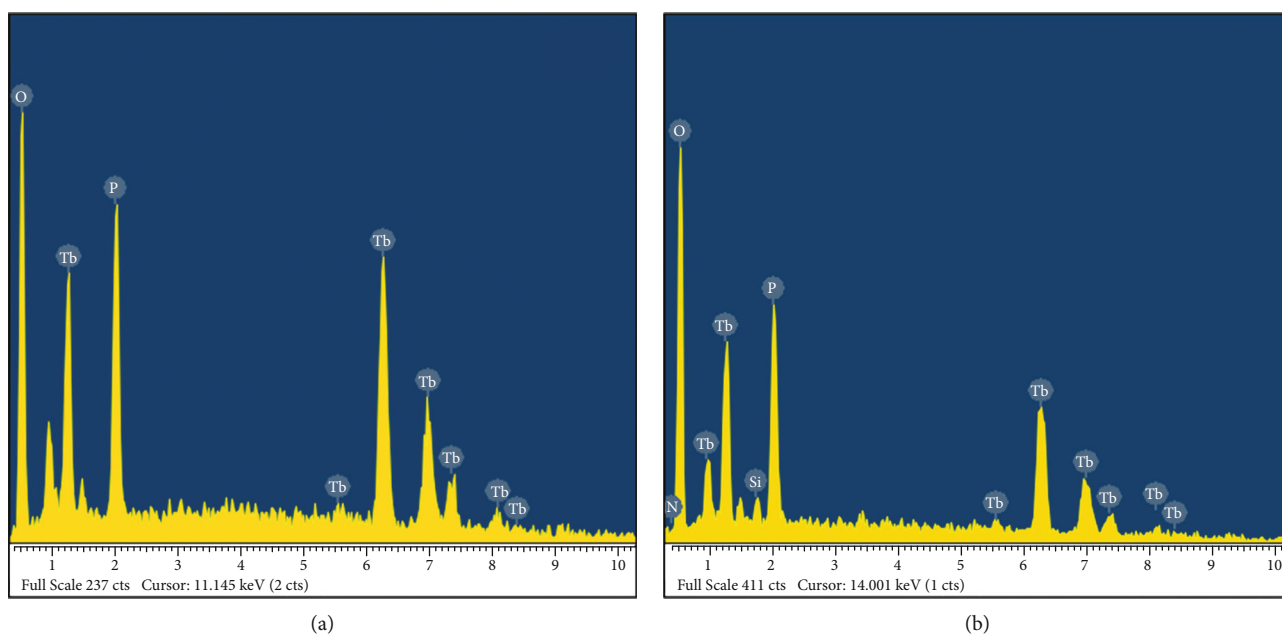


FIGURE 3: EDX spectra of the nanorods of $\text{TbPO}_4 \cdot \text{H}_2\text{O}$ (a) and $\text{TbPO}_4 \cdot \text{H}_2\text{O}@\text{silica-NH}_2$ (b).

$\text{TbPO}_4 \cdot \text{H}_2\text{O}@\text{silica-NH-folic acid}$ (2) is shown in Figure 4. The O-H vibrations were observed here as a shoulder at $\sim 3417 \text{ cm}^{-1}$. It can be observed that H_2O , Tb-O, PO_4^{3-} vibrations were defined at 1643 cm^{-1} , 951.8 cm^{-1} , and 670 cm^{-1} , respectively (Figure 4, line (1)).

After $\text{TbPO}_4 \cdot \text{H}_2\text{O}$ nanorods were protected with silica and then functionalized with amine and folic acid groups, there are three absorption peaks at 2091 cm^{-1} , 1643 cm^{-1} ,

and 1438 cm^{-1} corresponding to the vibrations of the N-H, C=O group [20, 23].

The asymmetric vibration of Si-O-Si is represented by strong absorption peaks at 1318 cm^{-1} and 1014 cm^{-1} (Figure 4, line (2)). Therefore, the information from infrared absorption spectroscopy proved clearly the existence of amine groups, Si-O-Si bond, and folic acid groups in the $\text{TbPO}_4 \cdot \text{H}_2\text{O}@\text{silica-NH-folic acid}$ nanorods. This also

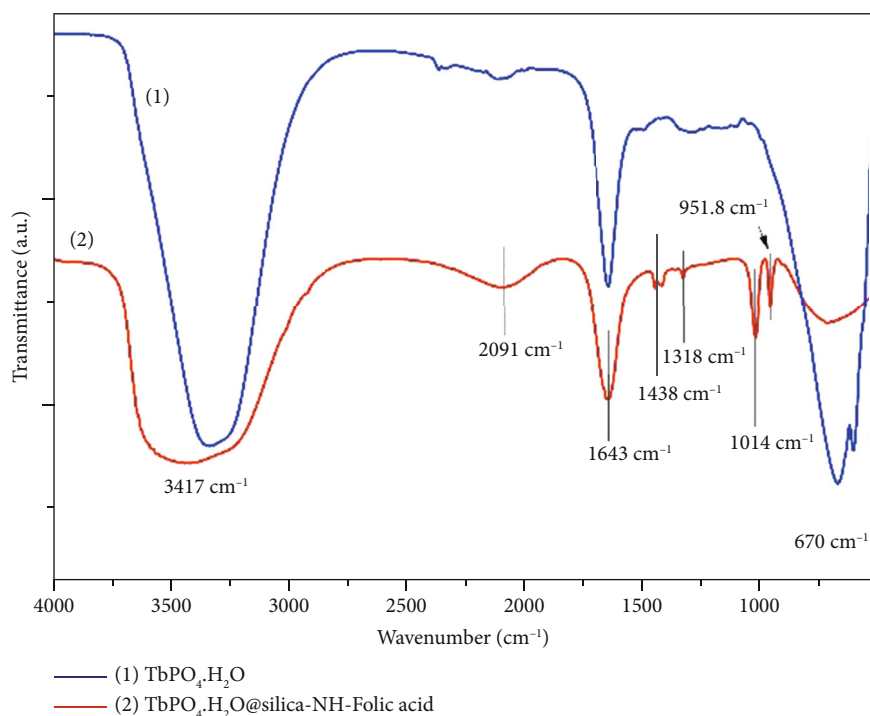


FIGURE 4: Fourier transform infrared spectra of the nanorods of $\text{TbPO}_4 \cdot \text{H}_2\text{O}$ (1) and $\text{TbPO}_4 \cdot \text{H}_2\text{O} @ \text{silica-NH-folic acid}$ (2).

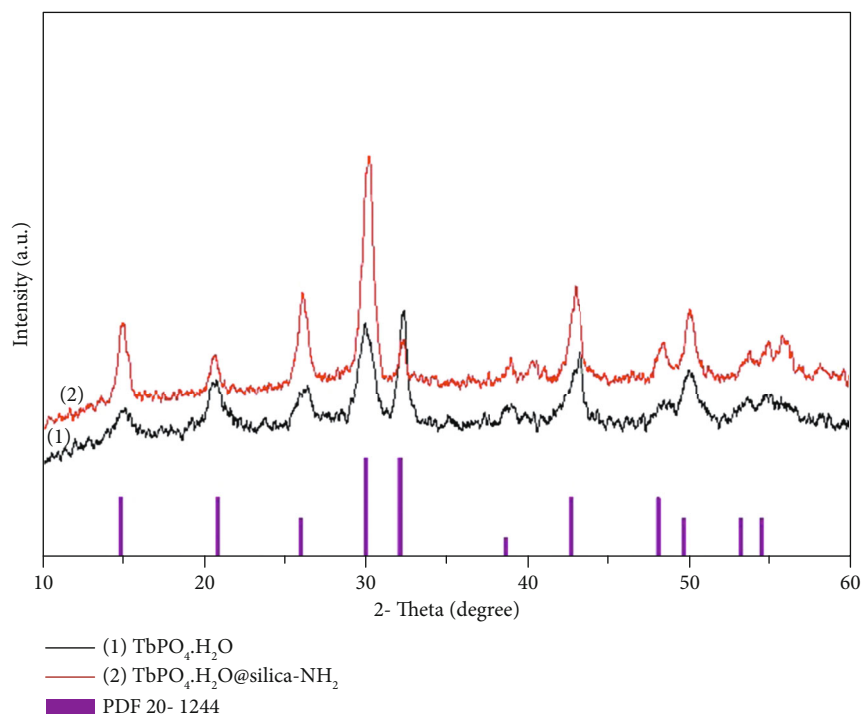


FIGURE 5: X-ray diffraction pattern of the nanorods of $\text{TbPO}_4 \cdot \text{H}_2\text{O}$ (line 1) and $\text{TbPO}_4 \cdot \text{H}_2\text{O} @ \text{silica-NH}_2$ (line 2) and standard data of hexagonal-phase $\text{TbPO}_4 \cdot \text{H}_2\text{O}$ (PDS card No. 20-1244) as a reference.

confirms the formation of linkage between the luminescence nanorods of $\text{TbPO}_4 \cdot \text{H}_2\text{O} @ \text{silica-NH}_2$ and the folic acid.

Figure 5 presents the X-ray diffraction pattern of the nanorods of $\text{TbPO}_4 \cdot \text{H}_2\text{O}$ (line 1), $\text{TbPO}_4 \cdot \text{H}_2\text{O} @ \text{silica-NH}_2$ (line 2), and standard data of hexagonal $\text{TbPO}_4 \cdot \text{H}_2\text{O}$ (space

group: $P3_121$, PDS card No. 20-1244, $a = 6.87 \text{ \AA}$; $c = 6.33 \text{ \AA}$) as a reference. We can see that the all diffraction peaks of the nanorods $\text{TbPO}_4 \cdot \text{H}_2\text{O}$ (line 1) and $\text{TbPO}_4 \cdot \text{H}_2\text{O} @ \text{silica-NH}_2$ (line 2) are high intensity, narrow width at 2θ angles of 14.85° , 20.83° , 25.95° , 30.01° , 32.10° , 38.75° , 42.78° , 48.13° ,

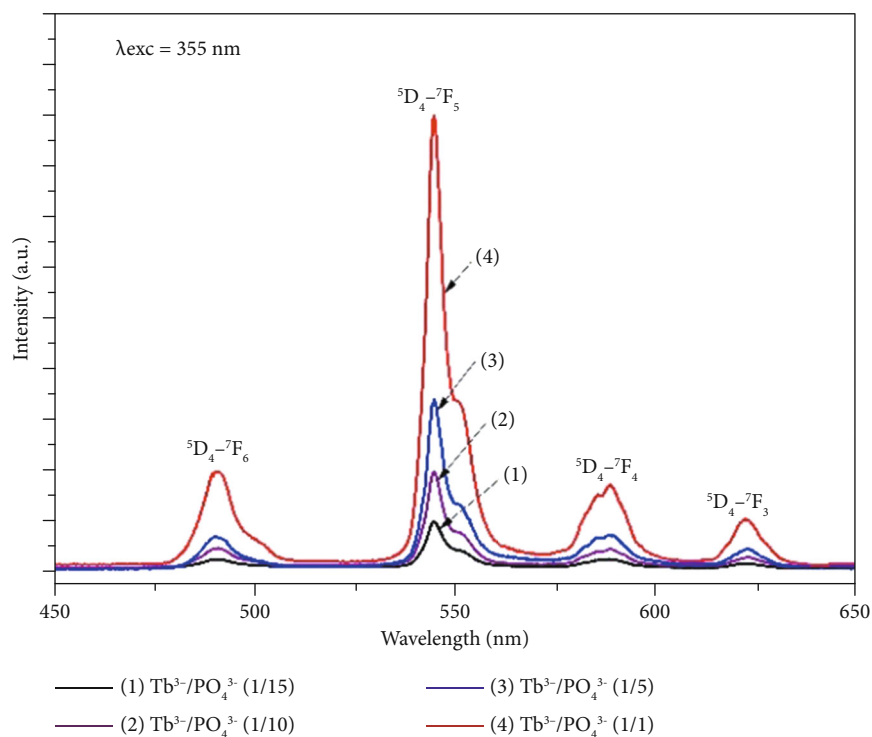


FIGURE 6: Photoluminescence spectra of the TbPO₄·H₂O samples with various molar ratios of Tb³⁺/PO₄³⁻: 1/15 (1); 1/10 (2); 1/5 (3); and 1/1(4).

49.70°, 53.21°, and 54.51°, and equivalent to the hexagonal phase of TbPO₄·H₂O (shown by PDF card No. 20-1244). This means both obtained TbPO₄·H₂O and TbPO₄·H₂O@silica-NH₂ nanorods are almost in a hexagonal phase form. The XRD results also revealed the amorphous nature of the shell layer (silica-NH₂) with no extra peaks was detected in these samples.

3.3. Photoluminescence Properties. Figure 6 shows the photoluminescence spectra of the TbPO₄·H₂O nanophosphors with various reactant Tb³⁺/PO₄³⁻ molar ratios under an excitation wavelength of 355 nm at the room temperature.

TbPO₄·H₂O nanophosphors exhibit the significant luminescence peaks at 488 nm, 540 nm, 585 nm, and 621 nm, which relate to ⁵D₄-⁷F₆, ⁵D₄-⁷F₅, ⁵D₄-⁷F₄, and ⁵D₄-⁷F₃ optical transitions of Tb³⁺, respectively. The results were achieved emission characteristics of Tb³⁺ from the TbPO₄·H₂O nanophosphor samples with different Tb³⁺/PO₄³⁻ molar ratios of 1/15 (line 1), 1/10 (line 2), 1/5 (line 3), and 1/1(line 4), in which the strongest emission peaks are yielded by the ⁵D₄-⁷F₅ transition at 540 nm (green light).

Moreover, we observed the increasing of TbPO₄·H₂O nanophosphor luminescence intensity when we raise up the amount of terbium nitrate in the synthesis. It seems that a highest luminescent intensity could be achieved in case of the synthesized TbPO₄·H₂O nanophosphors with the Tb³⁺/PO₄³⁻ molar ratio of 1/1. This result is evidence for there is no luminescent quenching effect occurring at the high concentration of Tb³⁺ in the synthesized nanophosphors.

Figure 7 shows the comparison of achieved photoluminescence spectra from TbPO₄·H₂O nanorods and TbPO₄·H₂O@

silica-NH-folic acid conjugate at 355 nm excitation wavelength. The luminescence peaks of TbPO₄·H₂O@silica-NH-folic acid conjugate appear at the same positions and remain a similar shape as TbPO₄·H₂O nanorod peaks. This result confirms that the luminescence properties of TbPO₄·H₂O nanorods have not changed after the functionalization and biological conjugation. Thus, these nanorods are very promising for biolabeling application.

3.4. In Vitro Cellular Imaging. A fluorescence microscope had been used for the observation tool to evaluate the linking ability between TbPO₄·H₂O@silica-NH-folic acid conjugates and MCF7 breast cancer cells after the incubation process described in the above experiment part. Figure 8 shows the fluorescent images for three cases: (a) MCF7 breast cancer cells (negative control), (b) incubated MCF7 breast cancer cells with TbPO₄·H₂O@silica-NH₂, and (c) incubated MCF7 breast cancer cells with TbPO₄·H₂O@silica-NH-folic acid; the concentration of 20 μg/ml for 3 hours was observed by the Olympus Scan^R 100X fluorescent microscope that used the excitation wavelength in the violet region (with filter ranged from 340 to 385 nm). For the first case, we did not observe luminescence emission in the reference sample (Figure 8(a)). In the second case, the incubated MCF7 breast cancer cells with TbPO₄·H₂O@silica-NH₂ sample shows low luminescence intensity (not bright) in Figure 8(b) that allow to propose about the weak bonds between TbPO₄·H₂O@silica-NH₂ and the cancer cells. The expected result has been achieved in the third case. We observed bright green pixels in Figure 8(c). This evidence demonstrates a strong coupling between MCF7 breast

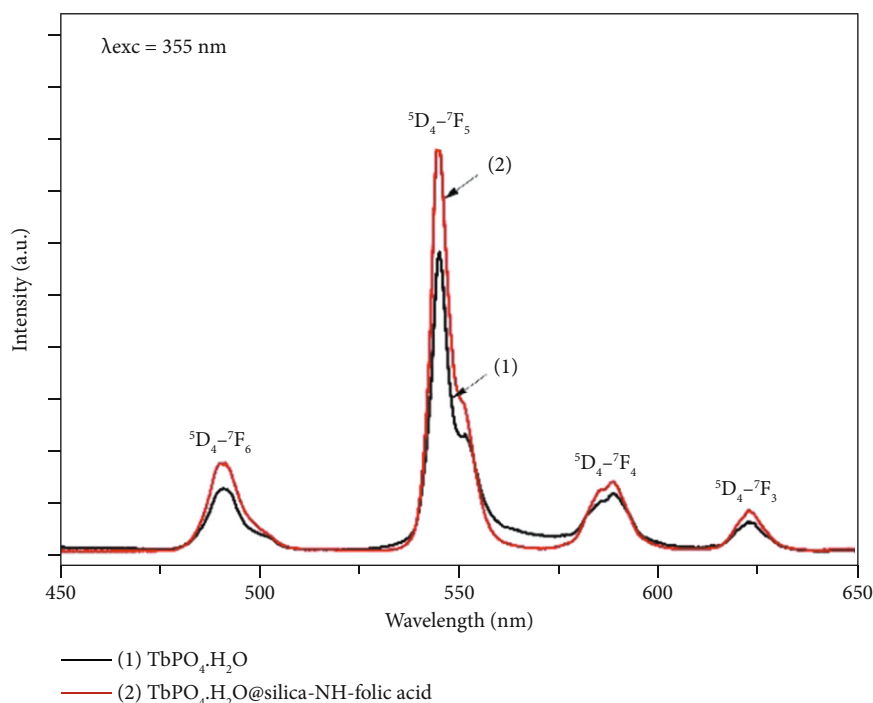


FIGURE 7: Photoluminescence spectra of $\text{TbPO}_4 \cdot \text{H}_2\text{O}$ nanorods (1) and $\text{TbPO}_4 \cdot \text{H}_2\text{O} @ \text{silica-NH-folic acid}$ (2) at $\lambda_{\text{exc}} = 355 \text{ nm}$.

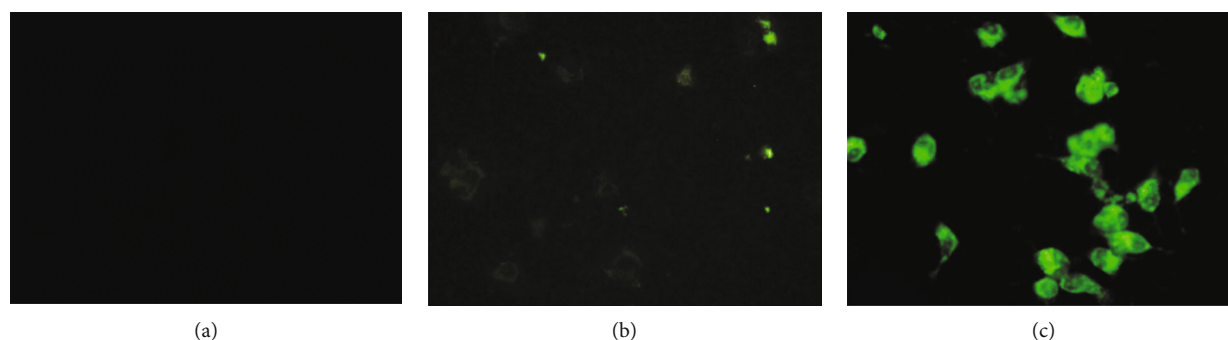


FIGURE 8: Fluorescent microscope images of MCF7 breast cancer cells after 3 hours of incubation with (a) negative control, (b) $\text{TbPO}_4 \cdot \text{H}_2\text{O} @ \text{silica-NH}_2$, and (c) $\text{TbPO}_4 \cdot \text{H}_2\text{O} @ \text{silica-NH-folic acid}$ conjugates with the concentration of $20 \mu\text{g/ml}$ were observed by the Olympus Scan[^]R 100X fluorescent microscope.

cancer cells and $\text{TbPO}_4 \cdot \text{H}_2\text{O} @ \text{silica-NH-folic acid}$ after we incubate these cells with the luminescence biological nanorod conjugates.

According to Soheila Kashanian, folic acid receptors are highly overexpressed on the surface of numerous tumour types including also breast cancer cells. Otherwise, folate receptors are selectively overexpressed in a number of tumour cell types but present in low or nondetectable levels in the most normal cells [24]. Our cellular images in Figure 8 shows clearly that the green emission of MCF7 breast cancer cells labeled with luminescent nanocomplex $\text{TbPO}_4 \cdot \text{H}_2\text{O} @ \text{silica-NH-folic acid}$ is much brighter (stronger luminescence) in comparison with the other reference cases, i.e., MCF7 breast cancer cells (negative control) or MCF7 breast cancer cells incubated with $\text{TbPO}_4 \cdot \text{H}_2\text{O} @ \text{silica-NH}_2$. In vitro cellular imaging tests have proved the localization of the functionalized $\text{TbPO}_4 \cdot \text{H}_2\text{O} @ \text{silica-NH-}$

folic acid within the cytoplasm of breast cancer cells. As seen in the fluorescence microscope images, the $\text{TbPO}_4 \cdot \text{H}_2\text{O} @ \text{silica-NH-folic acid}$ has localized within the cell cytoplasm. A short explanation for this result could be as follows. The high folic acid-folate receptor affinity allows the ligand binding between cell and luminescent labeling rod. After that, the $\text{TbPO}_4 \cdot \text{H}_2\text{O} @ \text{silica-NH-folic acid}$ has internalized into the cell via invagination process. Therefore, the $\text{TbPO}_4 \cdot \text{H}_2\text{O} @ \text{silica-NH-folic acid}$ could potentially use as biolabels for MCF-7 breast cancer cells. This test method based on fluorescent materials and a microscope could provide a quick tool to detect the cancer cells. In comparison with the other techniques, it is a nonsophisticated method without requirements of complex apparatus, e.g., spectral equipment and data analysis. Additionally, this provides a visual tool needed for some specific study in the biology.

4. Conclusions

We have successfully synthesized the uniform shape $\text{TbPO}_4\cdot\text{H}_2\text{O}$ nanorods with hexagonal phase using wet chemical methods. $\text{TbPO}_4\cdot\text{H}_2\text{O}$ @silica-NH-folic acid nanocomplex has been achieved by protecting these nanorods with silica layer, attaching with amine groups and then linking with folic acid by a coupling reaction. The sizes of this product were estimated at about 50–80 nm in the diameter and 500–800 nm in the length. The main characteristic emission bands of $\text{TbPO}_4\cdot\text{H}_2\text{O}$ @silica-NH-folic acid nanocomplex are located at 488 nm, 540 nm, 585 nm, and 621 nm regions in photoluminescence spectra, which attributed to the $^5\text{D}_4\text{-}^7\text{F}_j$ ($J = 6, 5, 4, 3$) transitions of Tb^{3+} ions, respectively, in which a very intense green luminescence peak at 540 nm has been observed. The preliminary in vitro test indicated that the $\text{TbPO}_4\cdot\text{H}_2\text{O}$ @silica-NH-folic acid nanocomplex could use for detecting and recognizing MCF7 breast cancer cells under a fluorescence microscope. This result allows us to propose $\text{TbPO}_4\cdot\text{H}_2\text{O}$ @silica-NH-folic acid nanocomplex as a very promising candidate with noncomplex apparatus for developing a quick fluorescent label and image tool in biomedicine.

Data Availability

The concerning data used to support the findings of this study are available from the corresponding author upon request.

Conflicts of Interest

The authors declare that there is no conflict of interest regarding the publication of this paper.

Acknowledgments

This work is funded by the Vietnamese Ministry of Education and Training under grant number B2019-MDA-04 and partly supported by the Institute of Materials Science, Vietnam Academy of Science and Technology under grant number CSPN.01/20-21.

References

- [1] A. Jain, P. G. J. Fournier, V. Mendoza-Lavaniegos et al., “Functionalized rare earth-doped nanoparticles for breast cancer nanodiagnostic using fluorescence and CT imaging,” *Journal of Nanobiotechnology*, vol. 16, no. 1, pp. 1–18, 2018.
- [2] M. Tan and G. Chen, “Rare earth-doped nanoparticles for advanced in vivo near infrared imaging,” in *Near Infrared-Emitting Nanoparticles for Biomedical Applications*, A. Benayas, E. Hemmer, G. Hong, and D. Jaque, Eds., pp. 63–81, Springer, Cham, 2020.
- [3] R. Yu, J. Bao, X. Yang et al., “Controlled synthesis of tetragonal terbium orthophosphate nanostructures through a solvothermal route,” *Research on Chemical Intermediates*, vol. 37, no. 2–5, pp. 145–151, 2011.
- [4] D. Giaume, M. Poggi, D. Casanova et al., “Organic functionalization of luminescent oxide nanoparticles toward their application as biological probes,” *Langmuir*, vol. 24, no. 19, pp. 11018–11026, 2008.
- [5] Z. Lihui, Y. Hongpeng, Y. Mei, and S. Yanhua, “Facile one-pot synthesis and luminescence of hexagonal $\text{TbPO}_4\cdot\text{nH}_2\text{O}$ hollow spheres,” *Materials Letters*, vol. 67, no. 1, pp. 256–258, 2012.
- [6] J. Bao, R. Yu, J. Zhang et al., “Controlled synthesis of terbium orthophosphate spindle-like hierarchical nanostructures with improved photoluminescence,” *European Journal of Inorganic Chemistry*, vol. 2009, no. 16, pp. 2388–2392, 2009.
- [7] T. T. Huong, H. T. Phuong, L. T. Vinh, H. T. Khuyen, T. K. Anh, and L. Q. Minh, “Functionalized $\text{YVO}_4\cdot\text{Eu}^{3+}$ nanophosphors with desirable properties for biomedical applications,” *Journal of Science: Advanced Materials and Devices*, vol. 1, no. 3, pp. 295–300, 2016.
- [8] Q. Fan, X. Cui, H. Guo, Y. Xu, G. Zhang, and B. Peng, “Application of rare earth-doped nanoparticles in biological imaging and tumor treatment,” *Journal of Biomaterials Applications*, vol. 35, no. 2, pp. 237–263, 2020.
- [9] E. Fanizza, N. Depalo, S. Fedorenko et al., “Green fluorescent terbium (III) complex doped silica nanoparticles,” *International Journal of Molecular Sciences*, vol. 20, no. 13, article 3139, pp. 1–16, 2019.
- [10] R. R. Zairov, A. O. Solovieva, N. A. Shamsutdinova et al., “Polyelectrolyte-coated ultra-small nanoparticles with Tb(III)-centered luminescence as cell labels with unusual charge effect on their cell internalization,” *Materials Science & Engineering. C, Materials for Biological Applications*, vol. 95, pp. 166–173, 2019.
- [11] J. Yang, G. Li, C. Peng et al., “Homogeneous one-dimensional structured $\text{Tb}(\text{OH})_3\cdot\text{Eu}^{3+}$ nanorods: hydrothermal synthesis, energy transfer, and tunable luminescence properties,” *Journal of Solid State Chemistry*, vol. 183, no. 2, pp. 451–457, 2010.
- [12] D. Yue, W. Lue, W. Lu et al., “A facile synthesis and optical properties of bundle-shaped $\text{TbPO}_4\cdot\text{H}_2\text{O}$ nanorods,” *Advances in Condensed Matter Physics*, vol. 2013, 5 pages, 2013.
- [13] C. R. Patra, R. Bhattacharya, S. Patra, S. Basu, P. Mukherjee, and D. Mukherjee, “Inorganic phosphate nanorods are a novel fluorescent label in cell biology,” *Journal of Nanobiotechnology*, vol. 4, no. 1, pp. 1–15, 2006.
- [14] K. L. Wong, G. L. Law, M. B. Murphy et al., “Functionalized europium nanorods for in vitro imaging,” *Inorganic Chemistry*, vol. 47, no. 12, pp. 5190–5196, 2008.
- [15] C. R. Patra, G. Alexandra, S. Patra et al., “Microwave approach for the synthesis of rhabdophane-type lanthanide orthophosphate ($\text{Ln} = \text{La, Ce, Nd, Sm, Eu, Gd}$ and Tb) nanorods under solvothermal conditions,” *New Journal of Chemistry*, vol. 29, no. 5, pp. 733–739, 2005.
- [16] F. Tao, Z. Wang, L. Yao, W. Cai, and X. Li, “Synthesis of $\text{Tb}(\text{OH})_3$ nanowire arrays via a facile template-assisted hydrothermal approach,” *Nanotechnology*, vol. 17, no. 4, pp. 1079–1082, 2006.
- [17] M. Yang, H. You, Y. Song et al., “Synthesis and luminescence properties of sheaflike TbPO_4 hierarchical architectures with different phase structures,” *Journal of Physical Chemistry C*, vol. 113, no. 47, pp. 20173–20177, 2009.
- [18] T. T. Huong, L. T. Vinh, T. K. Anh, H. T. Khuyen, H. T. Phuong, and L. Q. Minh, “Fabrication and optical characterization of multimorphological nanostructured materials containing $\text{Eu}(\text{III})$ in phosphate matrices for biomedical applications,” *New Journal of Chemistry*, vol. 38, no. 5, pp. 2114–2119, 2014.

- [19] A. A. Ansari, "Silica-modified luminescent LaPO₄:Eu@LaPO₄@SiO₂core/shell nanorods: synthesis, structural and luminescent properties," *Luminescence*, vol. 33, no. 1, pp. 112–118, 2018.
- [20] H. T. Phuong, T. T. Huong, L. T. Vinh et al., "Synthesis and characterization of NaYF₄:Yb³⁺,Er³⁺@silica-N=folic acid nanocomplex for bioimaginable detecting MCF-7 breast cancer cells," *Chung-kuo hsi t'u hsueh pao English Journal of the Chinese Rare Earth Society*, vol. 37, no. 11, pp. 1183–1187, 2019.
- [21] P. T. Lien, N. T. Huong, T. T. Huong et al., "Optimization of Tb³⁺/Gd³⁺ molar ratio for rapid detection of Naja Atra cobra venom by immunoglobulin G-conjugated GdPO₄·nH₂O : Tb³⁺ + Nanorods," *Journal of Nanomaterials*, vol. 2019, Article ID 3858439, 8 pages, 2019.
- [22] T. T. Huong, T. K. Anh, H. T. Khuyen, P. T. Hien, and L. Quoc Minh, "Fabrication and properties of terbium phosphate nanorods," *Advances in Natural Sciences: Nanoscience and Nanotechnology*, vol. 3, no. 1, p. 4.
- [23] T. M. Stauffer, *Applications of Molecular Spectroscopy to Current Research in the Chemical and Biological Sciences-Fourier Transform Infrared and Raman Characterization of Silica-Based Materials*, Larissa Brentano Capeletti and João Henrique Zimnoch, 2016, Intech, (Chapter 1).
- [24] H. Gomhor, J. Alqaraghuli, S. Kashanian, R. Rafipour, E. Mahdavian, and K. Mansouri, "Development and characterization of folic acid-functionalized apoferritin as a delivery vehicle for epirubicin against MCF-7 breast cancer cells," *artificial cells, Nanomedicine, and biotechnology*, vol. 46, no. sup3, pp. S847–S854, 2018.